COMPEL: The International Journal for Computation and Mathematics in Electrical and Electronic Engineering

Influence of non-linear frequency-dependent material properties on the operation of rotating electrical machines

Andreas Ruf Simon Steentjes David Franck Kay Hameyer

The current issue and full text archive of this journal is available on Emerald Insight at:
www.emeraldinsight.com/0332-1649.htm

Received 14 October 2014
Revised 21 January 2015
Accepted 22 January 2015

Influence of non-linear frequency-dependent material properties on the operation of rotating electrical machines

Andreas Ruf, Simon Steentjes, David Franck and Kay Hameyer
Institute of Electrical Machines, RWTH Aachen University, Aachen, Germany

Abstract

Purpose – The purpose of this paper is to focus on the frequency-dependent non-linear magnetization behaviour of the soft magnetic material, which influences both the energy loss and the performance of the electrical machine. The applied approach is based on measured material characteristics for various frequencies and magnetic flux densities. These are varied during the simulation according to the operational conditions of the rotating electrical machine. Therewith, the fault being committed neglecting the frequency-dependent magnetization behaviour of the magnetic material is examined in detail.

Design/methodology/approach – The influence of non-linear frequency-dependent material properties is studied by variation of the frequency-dependent magnetization characteristics. Two different non-oriented electrical steel grades having the same nominal losses at 1.5 T and 50 Hz, but different thickness, classified as M330-35A and M330-50A are studied in detail. Both have slightly different magnetization and loss behaviour.

Findings – This analysis corroborates that it is important to consider the frequency-dependency and saturation behaviour of the ferromagnetic material as well as its magnetic utilization when simulating electrical machines, i.e., its performance. The necessity to change the magnetization curve according to the applied frequency for the calculation of operating points depends on the applied material and the frequency range. Using materials, whose magnetization behaviour is marginally affected by frequency, causes a deviation in the flux-linkage and the electromagnetic torque in a small frequency range. However, analysing larger frequency ranges, the frequency behaviour of the material cannot be neglected. For instance, a poorer magnetizability requires a higher quadrature current to keep the same torque leading to increased copper losses. In addition, the applied iron-loss model plays a central role, since changes in magnetization behaviour with frequency lead to changes in the iron losses. In order to study the impact, the iron-loss model has to be capable to incorporate the harmonic content, because particularly the field harmonics are influenced by the shape of the magnetization curve.

Originality/value – This paper gives a close insight on the way the frequency-dependent non-linear magnetization behaviour affects the energy loss and the performance of electrical machines. Therewith measures to tackle this could be derived.

Keywords Electrical machine, PMSM, Magnetic hysteresis, Frequency-dependency, Magnetization curve, Operating range

Paper type Research paper

1. Introduction

The reliable estimation of energy loss in soft magnetic steel sheets and of the performance of electrical machines remains a much-discussed problem. This is supported by the pursuit of high power density machines operating as variable speed drives. Because of their wide frequency range driven by the demand of higher power density and its high magnetic utilization, the soft magnetic material modelling and machine design requires particular attention.

The results presented in this paper have been developed in a research project granted by the Federal Ministry for Economic Affairs and Energy with the reference number 01MY12006A.

COMPEL: The International Journal for Computation and Mathematics in Electrical and Electronic Engineering
Vol. 34 No. 3, 2015
pp. 674-690

0332-1649
DOI 10.1108/COMPEL-10-2014-0265

The magnetization behaviour of soft magnetic steel sheets is dependent on the applied frequency. However, in the Finite-Element (FE) models of electrical machines this frequency dependence is commonly not considered. Nowadays the commutation magnetization curve is applied for the simulation when using one magnetization curve (Bottauscio *et al.*, 2002), usually given for the frequency of 50 Hz. Hence, leaving the magnetization curve unchanged, the influence of the frequency is neglected (Bottauscio *et al.*, 2002).

On that account, this paper focusses on the frequency-dependent non-linear magnetization behaviour of the soft magnetic material, which influences both the energy loss and the performance of the electrical machine. The applied approach is based on measured material characteristics for various frequencies and magnetic flux densities. These are varied during the simulation according to the operational conditions of the rotating electrical machine. Therewith, the fault being committed neglecting the frequency-dependent magnetization behaviour of the magnetic material is examined in detail. Effects on torque, flux-linkage and iron losses are presented.

In this paper two different non-oriented electrical steel graded having the same nominal losses at 1.5 T and 50 Hz, but different thickness, classified as M330-35A and M330-50A are studied in detail.

Figure 1 depicts the measured magnetization curves of the investigated materials. These were obtained using standardized measurement equipment according to the IEC 60404 standard. Both have slightly different magnetization and loss behaviour. This is caused by both geometry-dependent induced eddy currents as well as microstructure-dependent excess eddy currents. The interdependence of macroscopic and microscopic eddy currents, hysteresis, skin-effect and magnetic saturation significantly affects the field distribution within the lamination and as a consequence the overall iron losses and magnetizability (Zirka *et al.*, 2008). Due to the changing dominating loss-mechanisms iron losses evolve in a different way with frequency and magnetic flux density.

From this characteristics a frequency-dependent behaviour of an electrical machine is expected. The purpose of this paper is to discuss the influence of the frequency-dependent material characteristics on the simulation results and the performance of the electrical machine. In addition, the iron-loss calculation is strongly influenced by the magnetization characteristics, which may lead to an inappropriate choice of the material employed in the machine. Two different models are used to calculate the iron-loss distribution in the electrical machine. A model corresponding to the state of the art and the other model which also considers the field harmonics within a period of the magnetic flux density.

The paper is structured as follows: Section 2 introduces the basic iron-loss calculation approaches applied to study the influence of various material grades and varying magnetization characteristics on the machines' iron losses. Subsequently, Section 3 presents the machine simulation methodology which enables to combine the material information (magnetization behaviour and iron losses) and the consideration of realistic operating conditions of electrical machines. The influence of magnetic material characteristics and iron-loss calculation approaches is briefly discussed in Section 4.

2. Iron-loss modelling

According to the well-known loss-separation principle (Bertotti 1998), the iron losses in electrical steel laminations can be separated into three parts:

(1) the Foucault eddy current losses, calculated in a macroscopic way with Maxwell's equations (Bertotti, 1998; Lammeraner and Štafl, 1966) assuming a homogeneous field distribution across the lamination thickness;

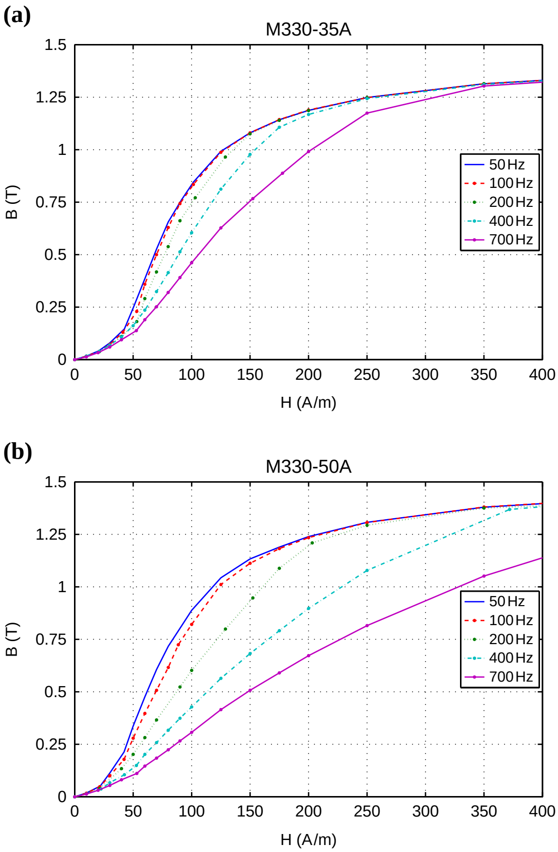

Figure 1.
Measured frequency-dependent magnetization curves

(2) the quasi-static hysteresis losses; and

(3) the excess (anomalous) losses, associated with the presence of domains, leading to various space-time dependencies in the magnetization process (Bertotti 1998).

It has been determined in Eggers *et al.* (2012) that the statistical three-term model underestimates the losses at high magnetic flux densities and high frequencies due to the neglection of the non-linear material behaviour. The classical Foucault eddy current loss term is a simplified description, valid under conditions where the magnetic field H within a thin lamination sheet shows a little deviation from the applied magnetic field H_a, i.e. $H \approx H_a$ (Bertotti 1998).

To overcome this, the Institute of Electrical machines proposed and validated a fourth loss term with a higher order B dependence. The mathematical formulation of the phenomenological model with higher order B term reads as follows:

$$P_{Fe} = a_1 B^{\alpha} f + a_2 B^2 f^2 (1 + a_3 B^{a_4}) + a_5 (Bf)^{1.5}, \quad (1)$$

where B is the magnetic flux density in Tesla (T), f the fundamental frequency in Hertz (Hz) and a_i, α material parameters.

Quasi-static hysteresis losses, classical Foucault eddy current losses and excess losses are included (respectively as terms with a_1, a_2 and a_5 coefficients), as well as the additional higher order B term, $a_3B^{a_4}$. In the first instance, the loss model is based on the fundamental frequency component and all a-parameters in Table I are identified using standardized Epstein measurement data (purely sinusoidal magnetic flux density waveforms) (Figure 2).

In general, the iron losses in soft magnetic materials are measured and theoretically estimated under specific, standardized conditions such as the Epstein test under uni-axial and purely sinusoidal magnetic flux density at 50 Hz and 1.0 T, respectively, 1.5 T (IEC 60404-2 and IEC 60404-3). However, magnetic flux paths occurring in rotating

Table I. Iron-loss model coefficients for both investigated electrical steel grades

Material	α	a_1	a_2	a_3	a_4	a_5
M330-35A	2.063	$18.249e^{-3}$	$51.513e^{-6}$	$170.984e^{-3}$	3.0	$0.47e^{-3}$
M330-50A	2.183	$11.501e^{-3}$	$89.491e^{-6}$	$134.517e^{-3}$	4.0	$0.941e^{-3}$

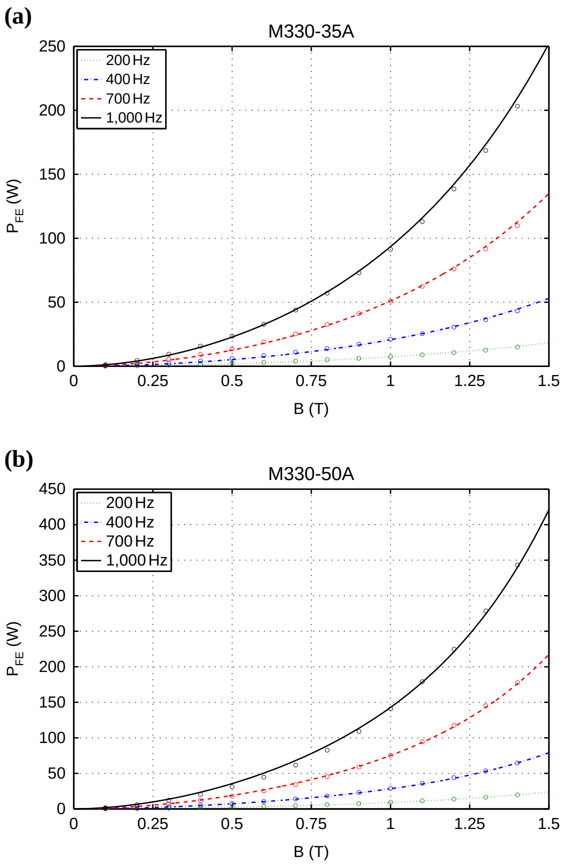

Figure 2. Comparison of calculated iron losses (1) with measurements at different frequencies using parameters of Table I

electrical machines are more complicated than in the case of standardized material characterization of Epstein strips. Field harmonics of the magnetic flux waveform occur due to iron saturation, skin-effect, stator and rotor slots. Together with harmonics in the excitation and supply currents, these lead to a significant increase of the iron losses. Furthermore, the different phenomenology of rotational losses requires to be considered. This paper utilizes two different extended iron-loss models based on (1).

A very powerful and fast method to obtain a general view of the iron losses in electrical machines is the utilization of the volumetric distribution of the maximal magnetic flux densities $B_{\max}$ over the FEs of the machine model during one magnetic period. Therewith, the losses can be calculated following (2) with contributions of quasi-static hysteresis losses (3), classical Foucault eddy current losses (4), excess eddy current losses (5) and saturation losses (6), where f is the fundamental frequency determined by the excitation current:

$$P_{\text{fund}} = P_{\text{hyst}} + P_{\text{classical}} + P_{\text{excess}} + P_{\text{sat}} \tag{2}$$

with the following loss contributions:

$$P_{\text{hyst}} = a_1\left(1+\frac{B_{\min}}{B_{\max}}(r_{\text{hyst}}-1)\right)B_{\max}^{\alpha}f \tag{3}$$

$$P_{\text{classical}} = a_2 B_{\max}^2 f^2 \tag{4}$$

$$P_{\text{excess}} = a_5\left(1+\frac{B_{\min}}{B_{\max}}(r_{\text{excess}}-1)\right)B_{\max}^{1.5}f^{1.5} \tag{5}$$

$$P_{\text{sat}} = a_2 a_3 B_{\max}^{a_4+2} f^2 \tag{6}$$

This formula is based on adding analytical, phenomenological descriptions to include the influence of rotational and flux distortion effects on the corresponding losses (Bertotti *et al.*, 1994; Steentjes *et al.*, 2012). Two parameters $B_{\min}$ and $B_{\max}$, respectively, the minimal and maximal magnetic flux density amplitudes over time, serve for this. This enables to identify the level of magnetic flux distortion by taking the ratio between $B_{\min}$ and $B_{\max}$. $B_{\max}$ gives an idea about the level of saturation. Zones with rotational hysteresis are those with large values of $B_{\min}$, whereas uni-directional field corresponds with a zero value of amplitude $B_{\min}$.

In order to consider the influence of induced field harmonics, the iron-loss model is extended by a Fourier series of the magnetic flux density waveform for the least common multiple of an electrical period and the rotational period of the rotor. Based on this, the amplitudes and orders of the field harmonics can be used for the iron-loss calculation (Bertotti *et al.*, 1994; Fiorillo and Novikov, 1990). The level of magnetic flux distortion and rotational magnetization are included in a similar way as previously described:

$$P_{Fe} = P_{\text{hyst}} + P_{\text{classical}} + P_{\text{excess}} + P_{\text{sat}} \tag{7}$$

with the following loss contributions:

$$P_{\text{hyst}} = a_1\left(1+\frac{B_{\min}}{B_{\max}}(r_{\text{hyst}}-1)\right)B_{\max}^{\alpha}f \tag{8}$$

$$P_{\text{classical}} = a_2 \sum_{n=1}^{\infty} \left(B_n^2 (nf)^2 \right) \tag{9}$$

$$P_{\text{excess}} = a_5 \left(1 + \frac{B_{\min}}{B_{\max}} (r_{\text{excess}} - 1) \right) \sum_{n=1}^{\infty} \left(B_n^{1.5} (nf)^{1.5} \right) \tag{10}$$

$$P_{\text{sat}} = a_2 a_3 B_{\max}^{a_4+2} f^2 \tag{11}$$

B_{n} is the amplitude of the n-th harmonic component of the magnetic flux density in Tesla (T), n the order of harmonic, f the fundamental frequency in Hertz (Hz), α, $a_1 - a_5$ the material specific parameters and r_{hyst}, r_{excess} the rotational loss factors (Steentjes *et al.*, 2012; Bertotti *et al.*, 1994).

The most sophisticated approach is to consider the operating range of the machine in addition. Therefore, a method is developed that allows combining efficiently the material information (loss and non-linear magnetization behaviour) with a FE model and the specific control strategy to incorporate the operation characteristics of the machine. This method involves an accurate computation of losses, including their separation into different components as well as an estimation of the effect of higher harmonics and rotational fields.

3. Methodology

The following section introduces a methodology to incorporate the operation characteristics in the simulation of electric machines. In order to evaluate the proposed methodology a permanent-magnet synchronous machine (PMSM) with buried magnets in the rotor and a rated power of 42.5 kW is studied (Finken *et al.*, 2010). The electrical machine is modelled in a rotor-flux-fixed dq-reference frame including cross coupling magnetization and saturation (Herold *et al.*, 2011):

$$\begin{bmatrix} \hat{\Psi}_{\text{d}} \\ \hat{\Psi}_{\text{q}} \end{bmatrix} = \begin{bmatrix} L_{\text{dd}} & L_{\text{dq}} \\ L_{\text{qd}} & L_{\text{qq}} \end{bmatrix} \begin{bmatrix} \hat{i}_{\text{d}} \\ \hat{i}_{\text{q}} \end{bmatrix} + \begin{bmatrix} \hat{\Psi}_{\text{f,d}} \\ \hat{\Psi}_{\text{f,q}} \end{bmatrix} \tag{12}$$

The quadrature and direct current is varied during the simulation to extract the average torque determined by the eggshell method (Henrotte *et al.*, 2004) for different excitations. The flux-linkage vector is calculated with the geometrical summation:

$$\hat{\Psi} = \sqrt{\hat{\Psi}_{\text{d}}^2 + \hat{\Psi}_{\text{q}}^2} \tag{13}$$

Figure 3 shows the result of the calculated average torque and flux-linkage for different dq-current excitations using FE simulation. In the case of a PMSM with buried magnets

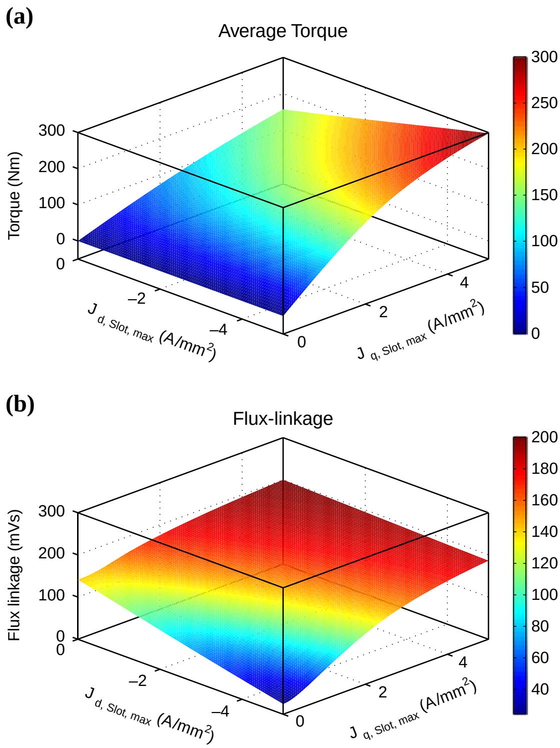

Figure 3.
Torque and flux-linkage in dq-reference frame

it is shown that the torque and the flux is strongly dependent on the amplitude and angle of the rotor-flux-fixed current vector.

In order to calculate the operating points for the whole operating range a combined control strategy is used. The optimization problem is defined by:

$$\begin{aligned} \underset{\hat{i}_{d,i,j},\hat{i}_{q,i,j}\in\mathbb{R}}{\text{minimize}} \quad & J(\hat{i}_{d,i,j},\hat{i}_{q,i,j}) = \sqrt{\hat{i}_{d,i,j}^2 + \hat{i}_{q,i,j}^2} \\ \text{subject to} \quad & T_i = \tfrac{3}{2}p\left(\hat{\Psi}_{d,i}\hat{i}_{q,i} - \hat{\Psi}_{q,i}\hat{i}_{d,i}\right), \quad \forall i = 1, \ldots, m. \\ & \hat{u}_j = \omega_j\hat{\Psi}_{d,i} \leqslant \hat{u}_{max}, \quad \forall j = 1, \ldots, n. \end{aligned}$$

with the torque vector $T_1, T_2, \ldots, T_m$ subject to $m \in \mathbb{N}$ and the speed vector $n_1, n_2, \ldots, n_n$ with $n \in \mathbb{N}$. This optimization problem combines the maximum torque per ampere (MTPA) control for the base speed range and the maximum torque per voltage (MTPV) control for the field weakening range (De Doncker *et al.*, 2010).

Figure 4 shows the trajectories of average electromagnetic torque calculated with different current excitations. Further an overlapping mesh of calculated operating points, from 0 to 533 Hz fundamental electrical frequency and 0 and 220 Nm inner electromagnetic

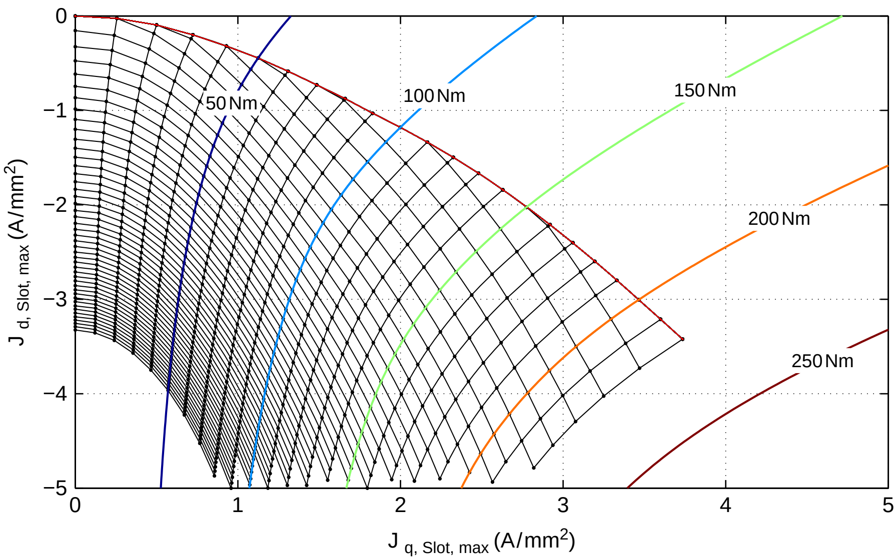

Figure 4. Simulated map of the average torque in Nm with overlapping mesh of operating points

torque, using the combined control strategy is mapped. The rotor-flux-fixed current vectors are defined for each operating point by the operating points, which are calculated for the given optimization problem. The basic speed range is represented by the trajectory that extends along the rising torques, whereas the field weakening area is represented by the mesh below this trajectory (Figure 4).

Figure 5 illustrates the direct and quadrature current component speed-torque map for the entire operating range for a maximum amplitude of the induced voltage of $\hat{u} = 360$ V.

The dq-current combination of these operating points directly depends on the harmonic electromagnetic torque and induced voltage, e.g., the differential of the flux-linkage at different stator currents, for the used control strategy.

In order to determine the influence of the frequency-dependent non-linear magnetization behaviour of the soft magnetic material, the electromagnetic torque and the flux-linkage are analysed for different magnetization curves and materials matching the fundamental frequency of the chosen operating point.

4. Results

4.1 Influence on calculation of operating points

The applied control strategy and operating points depend on the harmonic electromagnetic torque and the harmonic flux-linkage e.g. the induced voltage. Figure 6 shows the deviation between the obtained simulation results when using the respective 100 and 700 Hz magnetization curves to describe the magnetization characteristics of both materials.

The deviation increases for both materials in the negative d-axis, i.e., the field weakening range. The difference in q-current for the 0.35 mm thin material (M330-35A) is in the range of 1 per cent for all simulated stator currents. The difference increases using the 0.5 mm thin material (M330-50A) up to 2.5 per cent for the torque and

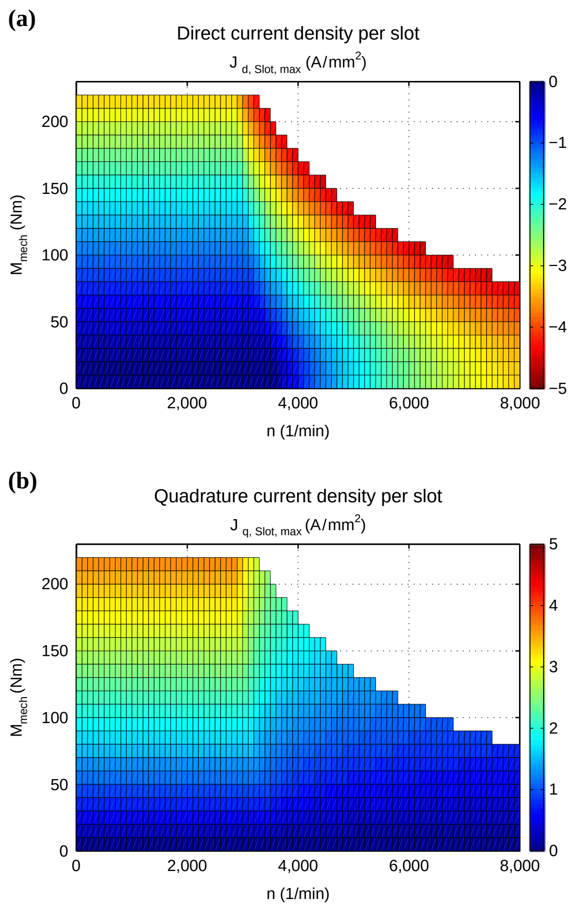

Figure 5.
Current density in dq-reference frame

1.2 per cent for the total harmonic flux-linkage. This result shows that the magnetization curve affects the calculation of the operating points for the considered PMSM depending on the chosen material.

In Figure 7 the influence on the calculation of operating points using different magnetization curves is illustrated for the 0.5 mm thin M330-50A grade. The variation of torque and flux-linkage, as shown in Figure 6(c) (d), has an impact on the amplitude and phase of the current vectors for various operating points. The reduced flux results in a reduction of the negative direct-current, because less field weakening is necessary. The most significant effect is caused by the lower torque affected by the magnetization curve measured at 700 Hz. The quadrature current is increased to provide the same torque. In Figure 7 (left) the two calculated meshes with operating points and (right) the deviation of the quadrature current are presented based on applying the 700 and 100 Hz magnetization curve for the 0.5 mm thin electrical steel grade. The most significant differences occur in the field weakening area, especially at lower torque. The deviation increases in this case up to 3 per cent for the quadrature current.

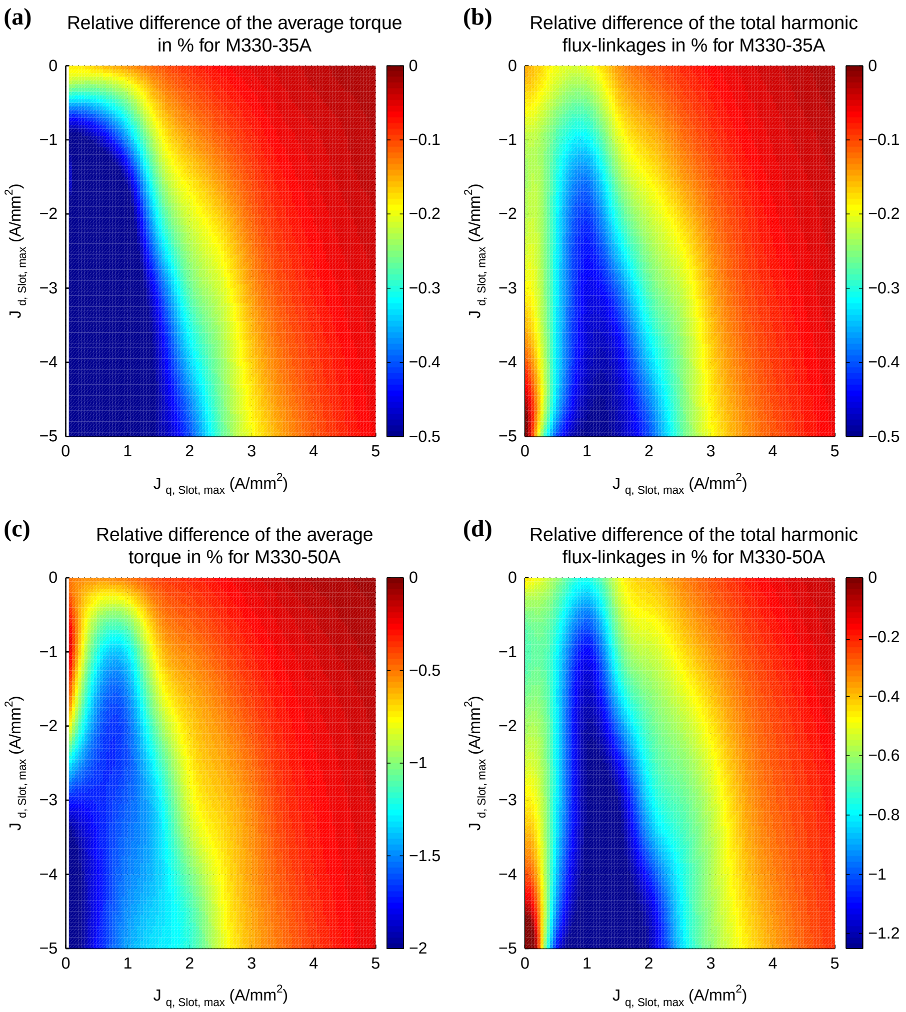

Figure 6. Deviation of torque (left) and magnetic flux (right) for two materials between results obtained using the 700 and 100 Hz magnetization curve with different stator currents

The impact of magnetization curves on the torque is shown in Figure 8 at the speed of 8,000 rpm. With the increase in the frequency of the magnetization curves the quadrature-current increases. The slope of this increase depends on the torque and decreases with increasing torque. However, this effect is strongly influenced by the rotational speed (Figure 7(b)).

These results show that the magnetization curve has an effect on the calculation of the operating points for the considered PMSM. This effect depends on the material used for the machine and on the state of saturation of the machine. High magnetic utilization and saturation characteristics of the magnetic material reduces this effect.

The effective operating points are identified considering the occurring losses, since the iron-loss calculation is directly dependent on the magnetization curve.

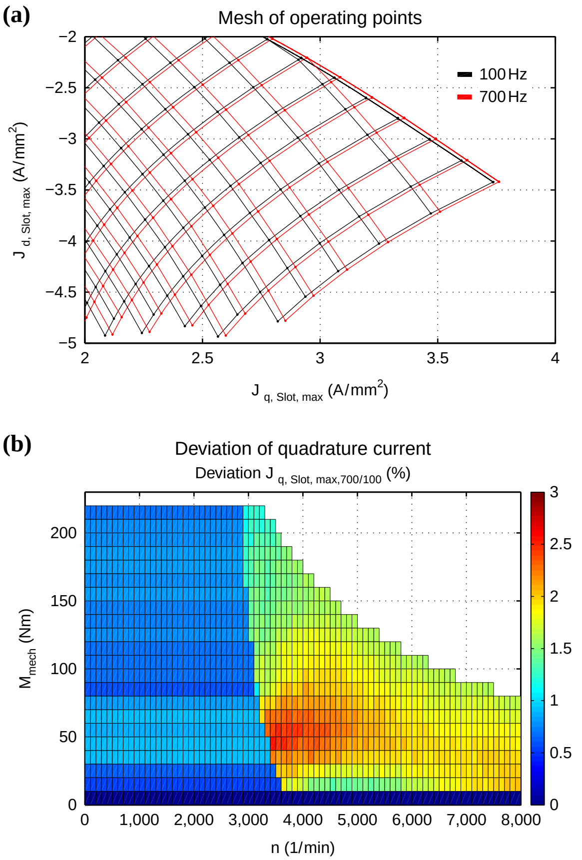

Figure 7.
Influence on the calculation of operating points using the 700 and 100 Hz magnetization curve for M330-50A

Subsequently the influence on the iron losses is examined using the IEM-loss-formula (Section 2), which allows a separation of the different loss components and its corresponding frequency order with consideration of rotating field vectors (Steentjes *et al.*, 2012). The calculated fault area is compared to the effective operating points at the corresponding frequency spectrum. The results are verified by the solutions for the elements in the 2D-mesh.

4.2 Influence on iron-loss calculation

In order to study the influence of frequency-dependent magnetization curves on the occurring iron losses, the iron-loss models, described in Section 2, are analysed for the 0.5 mm thin electrical steel grade, M330-50A.

The direct result of the FE simulation is the flux density distribution for each operation point. This distribution is directly influenced by the frequency-dependent material behaviour (Figure 1), in particular, at low and medium magnetic field strengths the magnetic flux density decreases due to the disturbing influence of induced eddy currents at higher excitation frequencies.

Figure 9(a) depicts the vectorial magnetic flux density distribution calculated using the 100 Hz magnetization curve, whereas Figure 9(b) shows the difference in

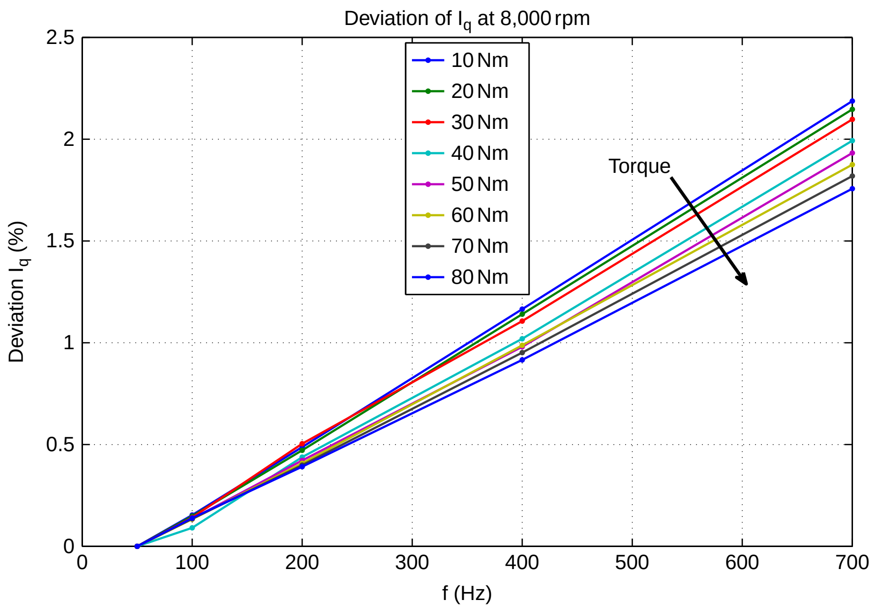

Figure 8. Deviation of quadrature current using different magnetization curves for different torques at the speed of 8,000 rpm

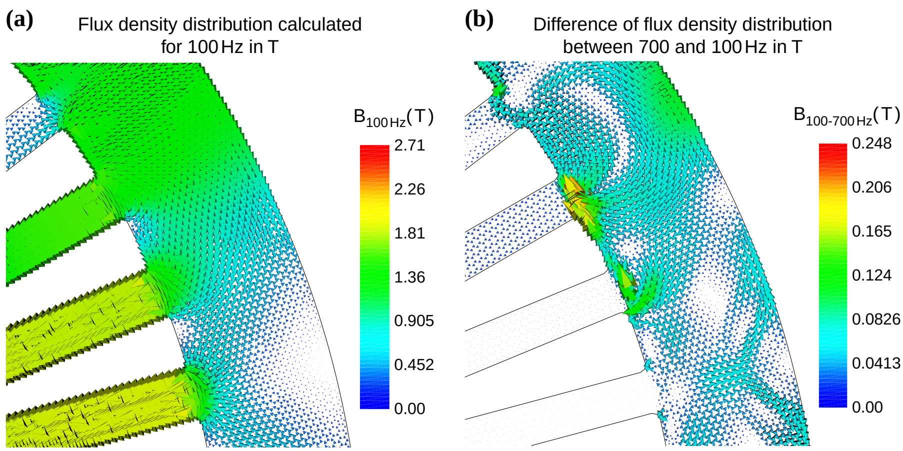

Figure 9. Effects on the magnetic flux density distribution calculated with different magnetization curves for M330-50A

flux density distributions between results obtained using the 700 Hz magnetization characteristic instead of the 100 Hz. It is apparentthat the difference in the entire cross-section for the considered material is small and, as a result of this, the effect on the torque as already shown (Figure 6(a) and (c)).

Subsequently, the influence of the material characteristics on the iron losses is analysed using the two loss models (2, 7) described in Section 2 (Steentjes *et al.*, 2012), which allow for loss-separation.

The relative differences (14) in calculated hysteresis losses (Figure 10), classical eddy current losses (Figure 11) and excess losses (Figure 12) using frequency-dependent

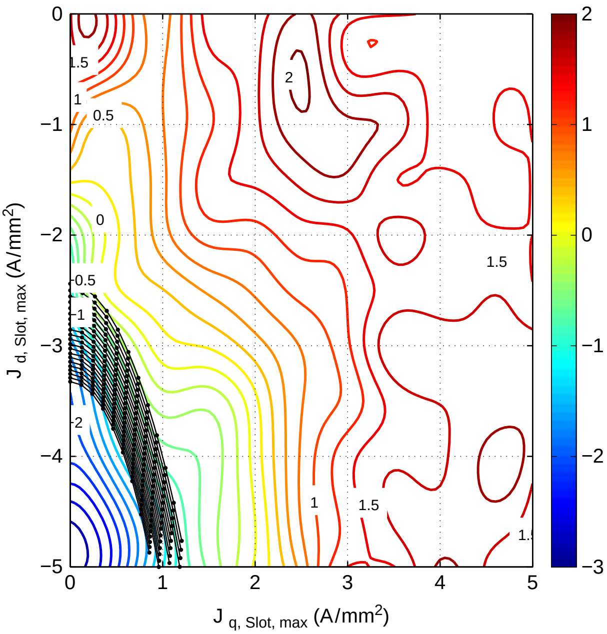

Figure 10. Relative difference of hysteresis losses in percentage between the FE simulations based on the 700 and 100 Hz magnetization curve

Note: Operating points are indicated as black dotted lines

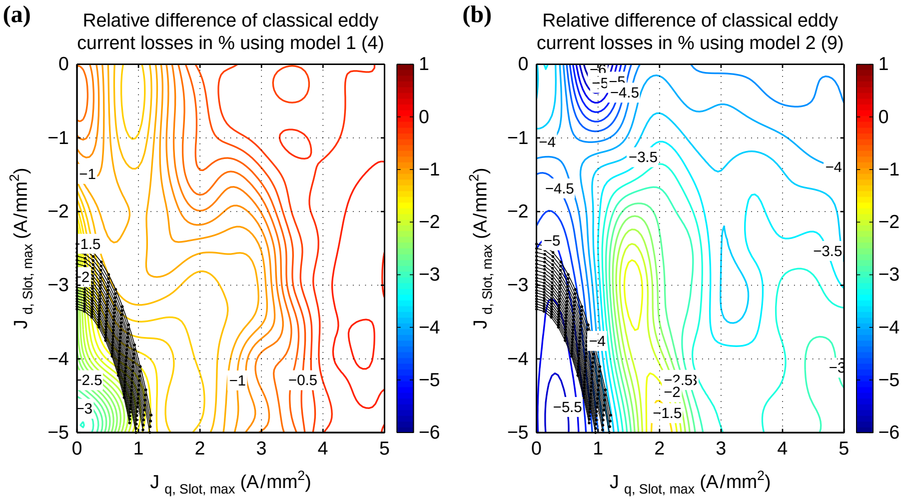

Figure 11. Deviation of classical eddy current losses between FE simulations based on 700 and 100 Hz magnetization curve

Note: Operating points are indicated as black dotted lines

magnetization curves corroborate the influence of the magnetization curve on the calculated iron losses:

$$p_{\text{hyst}} = \frac{P_{\text{hyst, 700 Hz}}}{P_{\text{hyst, 100 Hz}}}, \; p_{\text{classical}} = \frac{P_{\text{classical, 700 Hz}}}{P_{\text{classical, 100 Hz}}}, \; p_{\text{excess}} = \frac{P_{\text{excess, 700 Hz}}}{P_{\text{excess, 100 Hz}}} \tag{14}$$

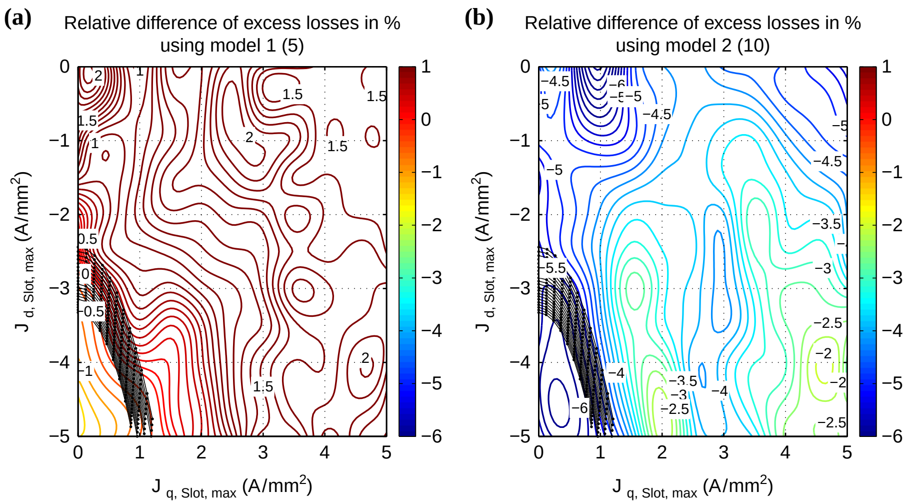

Note: Operating points are indicated as black dotted lines

Figure 12.
Deviation in percentage of excess losses between 700 and 100 Hz magnetization curve

The operating points indicated as black dotted curves in the various dq-current diagrams show the effective deviation, which is made using the magnetization curve of 100 Hz across the whole dq-range. The results for the first model are shown on the left side (a) and for the second model on the right side (b). The two models differ in their eddy and excess terms. The first model uses the maximum magnetic flux density B_{max} over the entire period of each FE, and the second model considers the field harmonics that occur during a period. Comparing the results in Figures 11 and 12 it becomes apparent that the first model has a smaller influence than the second model. In particular, the field harmonics are affected due to changes in the non-linear material behaviour. For this reason, it is necessary to use models for the iron-loss computation which consider harmonics in the flux density to reflect this influence. If the results are studied with regard to the indicated operating points at higher frequency a negative deviation occurs for all iron-loss components.

Looking on the whole dq-operation range the relative deviation lies between 2 and −2 per cent for the hysteresis losses (Model 1, 2) (Figure 10). For the classical eddy current losses Model 1 leads to a deviation which is between −0.5 and −3.5 per cent and Model 2 between −1.5 and −5.5 per cent (Figure 11). The excess losses have a deviation which is between 2 and −1 per cent (Model 1) and between −2.5 and −6 per cent (Model 2) (Figure 12). Particularly in regions where the flux density is low, e.g. in the yoke, the difference increases. As a result, the difference of the hysteresis and the classical eddy current loss distribution is shown in Figure 13. Both distributions show the negative deviation discussed above. At this frequency, e.g., operating point the classical eddy current losses are dominant. For this reason especially this loss component is important for the studied frequency-dependent influence and should be considered in the calculation of iron losses.

5. Conclusions

In this paper a methodology to study the influence of the non-linear frequency-dependent magnetic material behaviour on the operating characteristics of electrical machines,

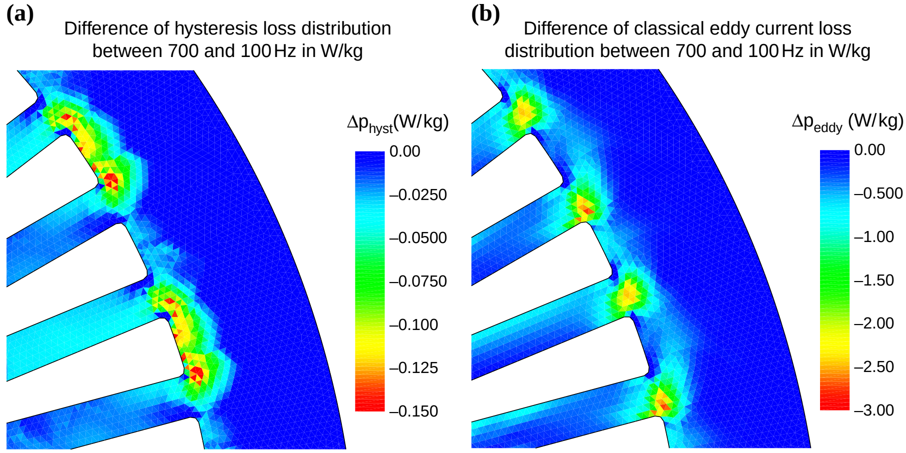

Figure 13. Difference of iron-loss distribution between 700 and 100 Hz magnetization curve at 7,000 rpm

in particular the iron losses, torque and flux-linkage is discussed. It has been shown that it is important to consider the frequency-dependency and saturation behaviour of the ferromagnetic material as well as its magnetic utilization, when selecting the most appropriate magnetic material for the application, e.g. an electric motor. The necessity to change the magnetization curve according to the applied frequency for the calculation of operating points depends on the applied material and the frequency range. Using materials, which magnetization curve is marginally affected by frequency, causes in a small frequency range an deviation in the flux-linkage and the electromagnetic torque which has an minor effect on the calculation of operating points. For larger frequency ranges, the frequency behaviour of the material can not be neglected. The reduction of the average torque requires a higher q-current to keep the same torque, which cause an increase in copper losses. The applied iron-loss model plays a central role, since the change in magnetization behaviour with frequency leads to a change in the iron-loss. To study this influence, the iron-loss model has to be capable to predict the harmonic content, because particularly the field harmonics are influenced by the shape of the magnetization curve.

References

Bertotti, G. (1998), *Hysteresis in Magnetism: For Physicists, Materials Scientists, and Engineers*, Academic Press, San Diego.

Bertotti, G., Canova, A., Chiampi, M., Chiarabaglio, D., Fiorillo, F. and Rietto, A. (1994), "Core loss prediction combining physical models with numerical field analysis", *Journal of Magnetism and Magnetic Materials*, Vol. 133 Nos 1-3, pp. 647-650.

Bottauscio, O., Canova, A., Chiampi, M. and Repetto, M. (2002), "Iron losses in electrical machines: influence of different material models", *IEEE Transactions on Magnetics*, Vol. 38 No. 2, pp. 805-808.

De Doncker, R., Pulle, D. and Veltman, A. (2010), *Advanced Electrical Drives: Analysis, Modeling, Control*, Springer, Berlin.

Eggers, D., Steentjes, S. and Hameyer, K. (2012), "Advanced iron-loss estimation for nonlinear material behavior", *IEEE Transactions on Magnetics*, Vol. 48 No. 11, pp. 3021-3024.

Finken, T., Hombitzer, M. and Hameyer, K. (2010), "Study and comparison of several permanent-magnet excited rotor types regarding their applicability in electric vehicles", *Emobility – Electrical Power Train*, pp. 1-7.

Fiorillo, F. and Novikov, A. (1990), "An improved approach to power losses in magnetic laminations under nonsinusoidal induction waveform", *IEEE Transactions on Magnetics*, Vol. 26 No. 5, pp. 2904-2910.

Henrotte, F., Deliége, G. and Hameyer, K. (2004), "The eggshell approach for the computation of electromagnetic forces in 2d and 3d", *COMPEL*, Vol. 23 No. 4, pp. 996-1005.

Herold, T., Franck, D., Lange, E. and Hameyer, K. (2011), "Extension of a D-Q model of a permanent magnet excited synchronous machine by including saturation, cross-coupling and slotting effects", *International Electric Machines and Drives Conference, IEMDC 2011, Niagara Falls, 15-18 May*.

Lammeraner, J. and Štafl, M. (1966), *Eddy Currents*, CRC Press, London.

Steentjes, S., Lessmann, M. and Hameyer, K. (2012), "Advanced iron-loss calculationas a basis for efficiency improvement of electrical machines in automotive application", *Proceedings of ESARS, Electrical Systems for Aircraft, Railway and Ship Propulsion (ESARS), Bologna, 16-18 October*.

Zirka, S.E., Moroz, Y.I., Marketos, P. and Moses, A.J. (2008), "Evolution of the loss components in ferromagnetic laminations with induction level and frequency", *Journal of Magnetism and Magnetic Materials*, Vol. 320 No. 20, pp. e1039-e1043.

About the authors

Andreas Ruf received the MSc Degree in Electrical Engineering from the Ruhr University Bochum (RUB), Germany, in August 2012. He has been working as a Research Associate at the Institute of Electrical Machines since January 2013. His research interests include iron loss computations, thermal behaviour, overload capability, lifetime models, the design and control of electrical machines. Andreas Ruf is the corresponding author and can be contacted at: Andreas.Ruf@iem.rwth-aachen.de

Simon Steentjes received the Diploma Degree in Electrical Engineering from the RWTH Aachen University, Germany, in November 2011. He has been working as a Research Associate at the Institute of Electrical Machines since December 2011. His research interests include hard- and soft magnetic material modelling on the micro- and macroscopic scale, iron loss calculation, effects of material processing, magnetic forces and mathematical methods.

David Franck received the Diploma degree in Electrical Engineering from the RWTH Aachen University, Aachen, Germany, in 2008. After that he became staff (Research Associate) at the Institute of Electrical Machines. Since 2011 he has been working as Chief Engineer of the Institute of Electrical Machines. His main field of research is the acoustic behaviour of electrical machines.

Dr Kay Hameyer received his MSc Degree in Electrical Engineering from the University of Hannover and his PhD Degree from the Berlin University of Technology, Germany. After his university studies he worked with the Robert Bosch GmbH in Stuttgart, Germany as a Design Engineer for permanent magnet servo motors and vehicle board net components. Until 2004 Dr Hameyer was a Full Professor for Numerical Field Computations and Electrical Machines with the KU Leuven in Belgium. Since 2004, he is a Full Professor and the director of the Institute of Electrical Machines (IEM) at RWTH Aachen University in Germany. 2006 he was the Vice Dean of the faculty and from 2007 to 2009 he was the Dean of the faculty of Electrical Engineering and Information Technology of RWTH Aachen University. His research interests are numerical field computation and optimization,

the design and controls of electrical machines, in particular permanent magnet excited machines, induction machines and the design employing the methodology of virtual reality. Since several years Dr Hameyer's work is concerned with the magnetic levitation for drive systems, magnetically excited audible noise in electrical machines and the characterization of ferromagnetic materials. Dr Hameyer is author of more than 250 journal publications, more than 500 international conference publications and author of four books. Dr Hameyer is a member of VDE, IEEE senior member, fellow of the IET.